# Layer-multiple-scattering theory for metamaterials made from clusters of nanoparticles

Vassilios Yannopapas* and Alexandros G. Vanakaras
*Department of Materials Science, University of Patras, GR-26504 Patras, Greece*
(Received 2 June 2011; revised manuscript received 29 July 2011; published 23 August 2011)

We present a layer-multiple-scattering method of electromagnetic waves for the study of periodic metamaterials formed as a lattice of cavities which are filled by clusters of spherical nanoparticles. Our approach is a three-stage process where we take fully into account all the multiple-scattering events involved: (a) among the spheres of the cluster inside the cavity, (b) between the cluster and the cavity, and (c) among the cavities (containing the clusters) within the metamaterial. As an example, we study the transmission, reflectance, and absorbance spectra of light incident on a finite slab of a $SiO_2$-inverted opal whose voids contain clusters of gold nanoparticles. We find, in particular, that finite slabs of this metamaterial act as highly efficient absorbers over a wide frequency range, from 2–4.5 eV. Also, around the local maxima of the absorbance spectrum, the metamaterial exhibits anomalous dispersion, wherein the real part of the group velocity is opposite to (the real part of) the phase velocity.

DOI: 10.1103/PhysRevB.84.085119 PACS number(s): 42.70.Qs, 42.25.Bs, 42.50.Gy, 78.67.Pt

## I. INTRODUCTION

Multiple scattering of waves by a collection of scatterers, apart from being a fundamental phenomenon in physics, constitutes a mathematical technique for solving the wave equation for given boundary conditions (those imposed by the presence of scatterers). For infinitely periodic arrays of scatterers, multiple-scattering theory has been formulated in different contexts, such as electrons in solids, electromagnetic (EM) waves in artificial dielectrics, and elastic waves in phononic structures. Multiple-scattering techniques are divided into two main categories: the bulk and the layer-multiple-scattering ones. In the bulk multiple-scattering theory, one deals with an infinitely periodic crystal and obtains the energy-band structure for electrons in atomic solids,[1] or the frequency band structure for classical (EM and elastic) waves.[2,3] In the layer-multiple-scattering (LMS) formulation, one assumes the periodic arrangement of scatterers in two dimensions (2D) offering the possibility for the study of various configurations, such as a single plane (monolayer) of scatterers, a finite slab of several planes or scatterers, or an infinitely periodic three-dimensional (3D) crystal viewed as a succession of planes parallel to a given crystallographic direction. For electrons in solids, the LMS method is widely known as the theory of low-energy electron diffraction (LEED),[4,5] while for photons[6–8] and phonons,[9] it is known as the EM and elastic LMS method, respectively. Apart from the obvious advantage of treating finite and infinite structures on an equal footing, the LMS method is an on-shell method and, as such, it provides a generally complex wave vector **k** of a 3D periodic structure for a given frequency or energy [the bulk multiple-scattering method provides the (real) frequency lines for a given (real) Bloch wave vector **k**]. The imaginary part of the wave vector defines the rate at which an incident beam is attenuated upon incidence on a finite slab of the crystal, if this is the case (within an energy or frequency band gap). Furthermore, the LMS formulation provides us with the transmission and reflection coefficients for a wave incident on a finite slab of the crystal (it also provides the absorption coefficient for the case of photons or phonons impinging on a lossy periodic structure). These coefficients are easily measured experimentally.

In the context of EM waves in artificial dielectrics, the LMS method has been employed for the study of photonic crystals and Mie-resonance-based metamaterials. Photonic crystals are manmade periodic structures in 2D or 3D with the period comparable to the wavelength of light, possessing an omnidirectional frequency band gap.[10,11] The latter is a result of the multiple interference of the EM waves within the photonic crystal. The LMS method, in particular, has been mainly used for the study of photonic crystals made by self-assembly, such as opal-based crystals. On the other hand, metamaterials are also manmade periodic structures, but their period is several times smaller than the wavelength of light. Due to this property, metamaterials mimic the response of a homogeneous medium and, by a properly chosen geometry of the scatterers comprising the (subwavelength) unit cell, they can exhibit exotic properties, such as artificial magnetism,[12] negative refractive index (NRI),[13] near-field amplification,[14] cloaking,[15] and perfect absorption.[16] Mie-resonance-based metamaterials are periodic structures consisting of scatterers of simple geometry, such as 2D arrays of cylinders[17,18] or 3D arrays of spherical particles,[19–28] exhibiting strong magnetic activity, as well as NRI in the microwave and infrared regimes (for a recent review, see Ref. 29). The emergence of artificial magnetism in Mie-resonance-based metamaterials relies on the excitation of Mie resonances on each individual particle of the metamaterial. The LMS method has been employed in metamaterials of spheres[20–28] supplemented by effective-medium theories.[30,31]

Recently, a bottom-up approach for realizing Mie-resonance-based metamaterials in the optical regime has been proposed,[32,33] wherein the required high-dielectric material is formed by the self-organization of metallic nanoparticles of few-nm radius. Such metamaterials have been realized by template-assisted, colloidal self-organization, wherein clusters of metallic nanoparticles reside within the voids of a 2D, periodically perforated, dielectric slab,[34] or within the trenches of a 1D grating.[35] The theoretical modeling of the above metamaterials relies on treating the EM response of the cluster of nanoparticles as a homogeneous body "cropped" out of an infinitely periodic metamaterial.[32–35] This approach is potentially valid only when the metallic nanoparticles are small enough (few nm) and the corresponding aggregates are

 

sufficiently large (several hundreds of nm) so that surface effects are negligible. For small aggregates containing tens or few hundreds of metallic nanoparticles, most particles reside at the surface of the cluster, rendering an effective-medium approach inadequate.

Motivated by the above structures, we present a first-principles study of the EM response of periodic structures of cavities containing clusters (aggregates) of nanoparticles by accurately taking into account all the multiple-scattering processes involved: (a) among the gold nanoparticles *within* the cluster, (b) between the cluster and the cavity, and (c) among the repeating units (cavity + nanocluster) of the metamaterial. The positions of the gold particles within the aggregates are taken from a rigorous Monte Carlo simulation of the self-organization of these particles, under the spherically confining potential of the cavity. The multiple-scattering theory of light within a single cavity + nanocluster provides a *total* scattering matrix. Having found the latter matrix, we embed it within the existing LMS formalism,[7,8] which provides us with the transmittance, reflectance, and absorbance of light incident on one or many two-dimensional lattices (planes) of clusters. Alternatively, the EM response can be studied by means of the complex frequency band structure of infinitely periodic metamaterials of clusters of particles. Besides the apparent application of the present work in metamaterials realized by template-assisted self-assembly, the formalism presented below constitutes a significant extension of the existing LMS formulations,[8,36] enabling the study of periodic structures with more than one scatterer in the 2D unit cell.

The paper is organized as follows: Sec. II describes the multiple-scattering theory followed for the study of the optical response of metamaterials consisting of cavities containing nanoparticle clusters. In Sec. III, we apply the method to the case of a silica-inverted opal containing clusters of gold nanoparticles in its voids, while Sec. IV concludes the paper.

## II. THEORY

### A. Multipole expansion of the EM field

Let us consider an harmonic EM wave of angular frequency $\omega$, which is described by its electric-field component,

$$\mathbf{E}(\mathbf{r},t) = \mathrm{Re}[\mathbf{E}(\mathbf{r})\exp(-\mathrm{i}\omega t)]. \tag{1}$$

In a homogeneous medium characterized by a dielectric function $\epsilon(\omega)\epsilon_0$ and a magnetic permeability $\mu(\omega)\mu_0$, where $\epsilon_0$ and $\mu_0$ are the electric permittivity and magnetic permeability of the vacuum, respectively, Maxwell equations imply that $\mathbf{E}(\mathbf{r})$ satisfies a vector Helmholtz equation, subject to the condition $\nabla\cdot\mathbf{E}=0$, with a wave number $q=\omega/c$, where $c=1/\sqrt{\mu\epsilon\mu_0\epsilon_0}=c_0/\sqrt{\mu\epsilon}$ is the velocity of light in the medium. The spherical-wave expansion of $\mathbf{E}(\mathbf{r})$ is given by[37]

$$\mathbf{E}(\mathbf{r}) = \sum_{l=1}^{\infty}\sum_{m=-l}^{l}\left\{a_{lm}^{H} f_l(qr)\mathbf{X}_{lm}(\hat{\mathbf{r}}) + a_{lm}^{E}\frac{\mathrm{i}}{q}\nabla\times[f_l(qr)\mathbf{X}_{lm}(\hat{\mathbf{r}})]\right\}, \tag{2}$$

where $a_{lm}^{P}$ $(P=E,H)$ are coefficients to be determined. $\mathbf{X}_{lm}(\hat{\mathbf{r}})$ are the so-called vector spherical harmonics,[37] and $f_l$ may be any linear combination of the spherical Bessel function $j_l$ and the spherical Hankel function $h_l^+$. The corresponding magnetic induction $\mathbf{B}(\mathbf{r})$ can be readily obtained from $\mathbf{E}(\mathbf{r},t)$ using Maxwell's equations,

$$\mathbf{B}(\mathbf{r}) = \frac{\sqrt{\epsilon\mu}}{c_0}\sum_{l=1}^{\infty}\sum_{m=-l}^{l}\left\{a_{lm}^{E} f_l(qr)\mathbf{X}_{lm}(\hat{\mathbf{r}}) - a_{lm}^{H}\frac{\mathrm{i}}{q}\nabla\times[f_l(qr)\mathbf{X}_{lm}(\hat{\mathbf{r}})]\right\}, \tag{3}$$

and we shall not write it down explicitly in what follows.

### B. Scattering by a single scatterer

In this section, we present a brief summary of the solution to the problem of EM scattering from a single sphere (Mie scattering theory),[37,38] along with an extension to the case of irregular (nonphysical) solutions, which are necessary for a wave emitted by the center of the sphere. We will make use of the compact notation of Ref. 39 for the eigenfunctions and the angular-momentum indices, which allows for easier computer coding.

We consider a sphere of radius $S$, with its center at the origin of coordinates, and assume that its electric permittivity $\epsilon_s$ and/or magnetic permeability $\mu_s$ are different from those $(\epsilon_h,\ \mu_h)$ of the surrounding homogeneous medium. An EM plane-wave incident on this scatterer is described, respectively, by Eq. (2) with $f_l=j_l$ (since the plane wave is finite everywhere) and appropriate coefficients $a_L^0$, where $L$ denotes collectively the indices $Plm$. That is,

$$\mathbf{E}^0(\mathbf{r}) = \sum_L a_L^0\mathbf{J}_L(\mathbf{r}), \tag{4}$$

where

$$\mathbf{J}_{Elm}(\mathbf{r}) = \frac{\mathrm{i}}{q_h}\nabla\times j_l(q_h r)\mathbf{X}_{lm}(\hat{\mathbf{r}}),\qquad \mathbf{J}_{Hlm}(\mathbf{r}) = j_l(q_h r)\mathbf{X}_{lm}(\hat{\mathbf{r}}), \tag{5}$$

and $q_h=\sqrt{\epsilon_h\mu_h}\omega/c_0$. The coefficients $a_L^0$ depend on the amplitude, polarization, and propagation direction of the incident EM plane wave.[7,8,37]

Similarly, the wave that is scattered from the sphere is described by Eq. (2) with $f_l=h_l^+$, which has the asymptotic form appropriate to an outgoing spherical wave: $h_l^+\approx(-\mathrm{i})^l\exp(\mathrm{i}q_h r)/\mathrm{i}q_h r$, as $r\to\infty$, and appropriate expansion coefficients $a_L^+$; namely,

$$\mathbf{E}^+(\mathbf{r}) = \sum_L a_L^+\mathbf{H}_L(\mathbf{r}), \tag{6}$$

where

$$\mathbf{H}_{Elm}(\mathbf{r}) = \frac{\mathrm{i}}{q_h}\nabla\times h_l^+(q_h r)\mathbf{X}_{lm}(\hat{\mathbf{r}}),\qquad \mathbf{H}_{Hlm}(\mathbf{r}) = h_l^+(q_h r)\mathbf{X}_{lm}(\hat{\mathbf{r}}). \tag{7}$$

The wave field for $r>S$ is the sum of the incident and scattered waves, i.e., $\mathbf{E}^{\mathrm{out}}=\mathbf{E}^0+\mathbf{E}^+$. The spherical-wave

expansion of the field $\mathbf{E}^I$ for $r < R$ (inside the sphere) is obtained in a similar manner by the requirement that it be finite at the origin ($\mathbf{r} = \mathbf{0}$), i.e.,

$$\mathbf{E}^I(\mathbf{r}) = \sum_L a_L^I \mathbf{J}_L^s(\mathbf{r}), \tag{8}$$

where $\mathbf{J}_L^s(\mathbf{r})$ are given from Eq. (5) by replacing $q_h$ with $q_s = \sqrt{\epsilon_s \mu_s}\omega/c_0$.

By applying the requirement that the tangential components of $\mathbf{E}$ and $\mathbf{H}$ be continuous at the surface of the scatterer, we obtain a relation between the expansion coefficients of the incident and the scattered field as follows:

$$a_L^+ = \sum_{L'} T_{LL'} a_{L'}^0, \tag{9}$$

where $T_{LL'}$ are the elements of the so-called scattering transition $T$ matrix.[38] Equation (9) is valid for any shape of scatterer; for spherically symmetric scatterers, each spherical wave scatters independently of all others, which leads to a transition $T$ matrix that does not depend on $m$ and is diagonal in $l$, i.e., $T_{LL'} = T_L \delta_{LL'}$. It is given by

$$T_{El}(\omega) = \left\{ \frac{j_l(q_s r)\frac{\partial}{\partial r}[r j_l(q_h r)]\,\epsilon_s - j_l(q_h r)\frac{\partial}{\partial r}[r j_l(q_s r)]\,\epsilon_h}{h_l^+(q_h r)\frac{\partial}{\partial r}[r j_l(q_s r)]\,\epsilon_h - j_l(q_s r)\frac{\partial}{\partial r}[r h_l^+(q_h r)]\epsilon_s} \right\}_{r=S}, \tag{10}$$

$$T_{Hl}(\omega) = \left\{ \frac{j_l(q_s r)\frac{\partial}{\partial r}[r j_l(q_h r)]\,\mu_s - j_l(q_h r)\frac{\partial}{\partial r}[r j_l(q_s r)]\,\mu_h}{h_l^+(q_h r)\frac{\partial}{\partial r}[r j_l(q_s r)]\,\mu_h - j_l(q_s r)\frac{\partial}{\partial r}[r h_l^+(q_h r)]\mu_s} \right\}_{r=S}. \tag{11}$$

The expansion coefficients $a_L^I$ of the field inside the spheres are given in terms of $a_L^0$ by a similar expression,

$$a_L^I = \sum_{L'} C_{LL'} a_{L'}^0. \tag{12}$$

The $C$ matrix is also independent of $m$ and diagonal in $l$, i.e., $C_{LL'} = C_L \delta_{LL'}$; it is given in terms of $T_{LL'}$:

$$C_{El}(\omega) = \sqrt{\frac{\epsilon_h \mu_s}{\epsilon_s \mu_h}}\left[\frac{j_l(q_h S)}{j_l(q_s S)} + \frac{h_l^+(q_h S)}{j_l(q_s S)} T_{El}\right], \tag{13}$$

$$C_{Hl}(\omega) = \frac{j_l(q_h S)}{j_l(q_s S)} + \frac{h_l^+(q_h S)}{j_l(q_s S)} T_{Hl}. \tag{14}$$

In a similar manner, one can define a wave which is infinite at the origin and matches continuously an outgoing spherical wave of given $L$ outside the sphere. For this purpose, the electric field outside the sphere is written as

$$\mathbf{E}^0(\mathbf{r}) = \sum_L b_L^0 \mathbf{H}_L(\mathbf{r}), \tag{15}$$

and inside the sphere as

$$\mathbf{E}^I(\mathbf{r}) = \sum_L \left[b_L^I \mathbf{J}_L^s(\mathbf{r}) + b_L^{I+} \mathbf{H}_L^s(\mathbf{r})\right], \tag{16}$$

where $\mathbf{H}_L^s(\mathbf{r})$ is given by Eq. (7) with $q_s$ instead of $q_h$. Again, by requiring that the tangential components of the electric and magnetic fields be continuous on the surface of the sphere, one can express $b_L^I$ and $b_L^{I+}$ in terms of $b_L^0$ as follows:

$$b_L^{I+} = \sum_{L'} Q_{LL'} b_{L'}^0, \quad b_L^I = \sum_{L'} P_{LL'} b_{L'}^0, \tag{17}$$

where, similar to the $T$ matrix, $Q_{LL'}$ and $P_{LL'}$ are diagonal in $l$ and do not depend on $m$. They are provided by

$$Q_{El}(\omega) = \sqrt{\frac{\epsilon_h \mu_s}{\epsilon_s \mu_h}}\left[\frac{h_l^+(q_h S)}{h_l^+(q_s S) + j_l(q_s S) V_{El}}\right], \tag{18}$$

$$Q_{El}(\omega) = \frac{h_l^+(q_h S)}{h_l^+(q_s S) + j_l(q_s S) V_{Hl}}, \tag{19}$$

$$P_{El}(\omega) = V_{El} Q_{El}, \tag{20}$$

$$P_{Hl}(\omega) = V_{Hl} Q_{Hl}, \tag{21}$$

and

$$V_{El}(\omega) = \left\{ \frac{h_l^+(q_s r)\frac{\partial}{\partial r}[r h_l^+(q_h r)]\epsilon_s - h_l^+(q_h r)\frac{\partial}{\partial r}[r h_l^+(q_s r)]\epsilon_h}{h_l^+(q_h r)\frac{\partial}{\partial r}[r j_l(q_s r)]\,\epsilon_h - j_l(q_s r)\frac{\partial}{\partial r}[r h_l^+(q_h r)]\epsilon_s} \right\}_{r=S}, \tag{22}$$

$$V_{Hl}(\omega) = \left\{ \frac{h_l^+(q_s r)\frac{\partial}{\partial r}[r h_l^+(q_h r)]\mu_s - h_l^+(q_h r)\frac{\partial}{\partial r}[r h_l^+(q_s r)]\mu_h}{h_l^+(q_h r)\frac{\partial}{\partial r}[r j_l(q_s r)]\,\mu_h - j_l(q_s r)\frac{\partial}{\partial r}[r h_l^+(q_h r)]\mu_s} \right\}_{r=S}. \tag{23}$$

### C. Multiple scattering by a collection of spheres

Next we consider a collection of $N_s$ nonoverlapping spherical scatterers centered at sites $\mathbf{R}_n$ in a homogeneous host medium. An outgoing vector spherical wave about $\mathbf{R}_{n'}$ can be expanded in a series of incoming vector spherical waves around $\mathbf{R}_n$ as follows:

$$\mathbf{H}_{L'}(\mathbf{r} - \mathbf{R}_{n'}) = \sum_L \Omega_{LL'}^{nn'} \mathbf{J}_L(\mathbf{r} - \mathbf{R}_n). \tag{24}$$

An outgoing vector spherical wave about $\mathbf{R}_{n'}$ can be expanded in a series of outgoing vector spherical waves around $\mathbf{R}_n$ as follows:

$$\mathbf{H}_{L'}(\mathbf{r} - \mathbf{R}_{n'}) = \sum_L \Xi_{LL'}^{nn'} \mathbf{H}_L(\mathbf{r} - \mathbf{R}_n), \tag{25}$$

and similarly for incoming vector spherical waves,

$$\mathbf{J}_{L'}(\mathbf{r} - \mathbf{R}_{n'}) = \sum_L \Xi_{LL'}^{nn'} \mathbf{J}_L(\mathbf{r} - \mathbf{R}_n). \tag{26}$$

Explicit formulas for the matrices $\mathbf{\Omega}$ and $\Xi$ are given in the Appendix. These matrices do not depend on the material properties of the scatterers, but on their particular arrangement in space. From Eq. (24), we can express an outgoing EM wave about $\mathbf{R}_{n'}$, $\sum_{L'} b_{L'}^{+n'} \mathbf{H}_{L'}(\mathbf{r}-\mathbf{R}_{n'})$, to an incoming EM wave about $\mathbf{R}_n$, $\sum_L b_L^{'n} \mathbf{J}_L(\mathbf{r}-\mathbf{R}_n)$, as follows:

$$b_L^{'n}(n') = \sum_{L'} \Omega_{LL'}^{nn'} b_{L'}^{+n'}. \tag{27}$$

The wave scattered from the sphere at $\mathbf{R}_n$ is determined by the total incident wave on this sphere, i.e.,

$$b_L^{+n} = \sum_{L'} T_{LL'}^n \left[ a_{L'}^{0n} + \sum_{n' \neq n} b_{L'}^{'n}(n') \right], \tag{28}$$

where $T_{LL'}^n = T_L^n \delta_{LL'}$ is the $T$ matrix for the sphere at $\mathbf{R}_n$, and $a_L^{0n}$ are the spherical-wave expansion coefficients of an externally incident wave. Equation (28) can be written as

$$\sum_{n'L'} \left[ \delta_{nn'}\delta_{LL'} - \sum_{L''} T_{LL''}^n \Omega_{L''L'}^{nn'} \right] b_{L'}^{+n'} = \sum_{L'} T_{LL'}^n a_{L'}^{0n}. \tag{29}$$

The above equation is the basic equation of multiple scattering and can be solved by standard linear-system numerical solvers, or iteratively.[40] The solution provides the scattering wave $b_L^{+n}$ outgoing from each sphere of the collection for a given externally incident wave $a_L^{0n}$. Having calculated $b_L^{+n}$ from Eq. (29), one can readily find the coefficients $b_L^{'n}(n')$ from Eq. (27) and therefore the total incident wave to each sphere of the collection given by the square brackets of Eq. (28). Using the total incident wave as input to Eq. (12), one can determine the multipole coefficients $a_L^{I\,n}$ within each sphere of the collection. The corresponding electric field is given similar to Eq. (16).

The electric field outside the spheres, $\mathbf{E}^{\text{out}}$, is written as the sum of the scattered field from all spheres plus the incident wave field, i.e.,

$$\mathbf{E}^{\text{out}}(\mathbf{r}) = \mathbf{E}^{sc}(\mathbf{r}) + \mathbf{E}^0(\mathbf{r}), \tag{30}$$

where the incident field $\mathbf{E}^0$ is given by Eq. (4), and $\mathbf{E}^{sc}$ is given as follows:

$$\mathbf{E}^{sc}(\mathbf{r}) = \sum_{n=1}^{N_s} \sum_{L} b_L^{+n} \mathbf{H}_L(\mathbf{r}-\mathbf{R}_n). \tag{31}$$

In order to incorporate a cluster of spherical scatterers within the existing LMS code as a single-scattering entity, we need to calculate the scattering $T$ matrix $T_{LL'}^{\text{cl}}$ of the entire cluster. It can be shown that the scattering matrix $T_{LL'}^{\text{cl}}$ assumes the form[39]

$$T_{LL'}^{\text{cl}} = \sum_{nn'} \sum_{L''L'''} \Xi_{LL''}^{0n} [(\mathbf{I} - \mathbf{T}\Omega)^{-1}\mathbf{T}]_{L''L'''}^{nn'} \Xi_{L'''L'}^{n'0}, \tag{32}$$

where the matrix $(\mathbf{I} - \mathbf{T}\Omega)$ is the one appearing on the left-hand side of Eq. (29). $T_{LL'}^{\text{cl}}$ contains nondiagonal elements in general. We note that alternative formulations of the EM scattering by a finite number of scatterers have been developed in the past.[41] However, the formalism presented above is suitable for embedding the $T$ matrix of Eq. (32) in the existing LMS formalism.

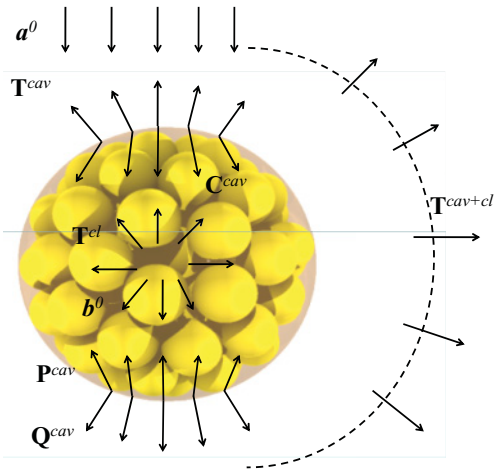


FIG. 1. (Color online) Matrices involved for the calculation of the total scattering matrix $\mathbf{T}^{\text{cav+cl}}$ of a cluster of particles within a cavity. A plane wave (corresponding to multipole coefficients $a^0$) incident on the cavity (without the cluster) is either scattered off of the cavity via $\mathbf{T}^{\text{cav}}$ or enters the cavity via $\mathbf{C}^{\text{cav}}$. A spherical wave (corresponding to multipole coefficients $b^0$) outgoing from the center of the cavity is either scattered back at the boundary of the cavity via $\mathbf{P}^{\text{cav}}$ or escapes the cavity via $\mathbf{Q}^{\text{cav}}$. The scattering matrix of the cluster is $\mathbf{T}^{\text{cl}}$.

### D. Multiple scattering in a spherical cavity

We assume that a cluster of scatterers described by a $T$matrix, $T^{\text{cl}}$, is embedded within a spherical cavity (see Fig. 1), which is associated with a scattering matrix, $T^{\text{cav}}$. The system of the cavity containing the cluster of scatterers is illuminated by a wave of the form of Eq. (4) with multipole coefficients $a_L^0$. This wave can be directly scattered off of the cavity, producing an outgoing wave of the form of Eq. (6) with multipole coefficients $a_L^+$ given by

$$a_L^+ = \sum_{LL'} T_{LL'}^{\text{cav}} a_{L'}^0, \tag{33}$$

or it can enter the cavity producing a wave in the manner of Eq. (12),

$$\sum_{LL'} C_{LL'}^{\text{cav}} a_{L'}^0, \tag{34}$$

which is incident on the cluster of scatterers. The above wave is scattered off the cluster via $\mathbf{T}^{\text{cl}}$ and then escapes the cavity via the matrix $\mathbf{Q}^{\text{cav}}$ [first of Eqs. (17)]. So, the second contribution to the scattering waves of the cavity + nanocluster amounts to

$$\sum_{L'} [\mathbf{Q}^{\text{cav}}\mathbf{T}^{\text{cl}}\mathbf{C}^{\text{cav}}]_{LL'} a_{L'}^0. \tag{35}$$

However, the wave outgoing from the cluster $\sum_{L'} [\mathbf{T}^{\text{cl}}\mathbf{C}^{\text{cav}}]_{LL'} a_{L'}^0$ can be scattered at the inner surface of the cavity and return back to the cluster via the matrix $\mathbf{P}^{\text{cav}}$ [second of Eqs. (17)], producing in this way a new incident field on the cluster. The latter is again scattered off of the cluster via $\mathbf{T}^{\text{cl}}$ and escapes the cavity via $\mathbf{Q}^{\text{cav}}$, producing a wave of the form

$$\sum_{L'} [\mathbf{Q}^{\text{cav}}\mathbf{T}^{\text{cl}}\mathbf{P}^{\text{cav}}\mathbf{T}^{\text{cl}}\mathbf{C}^{\text{cav}}]_{LL'} a_{L'}^0. \tag{36}$$

It can be easily understood that this process can be repeated infinite times, giving rise to a series of multiple-scattering events:

$$\begin{aligned}&\sum_{L'}[\mathbf{Q}^{\mathrm{cav}}\mathbf{T}^{\mathrm{cl}}\mathbf{C}^{\mathrm{cav}}+\mathbf{Q}^{\mathrm{cav}}\mathbf{T}^{\mathrm{cl}}\mathbf{P}^{\mathrm{cav}}\mathbf{T}^{\mathrm{cl}}\mathbf{C}^{\mathrm{cav}}\\&\quad+\mathbf{Q}^{\mathrm{cav}}\mathbf{T}^{\mathrm{cl}}\mathbf{P}^{\mathrm{cav}}\mathbf{T}^{\mathrm{cl}}\mathbf{P}^{\mathrm{cav}}\mathbf{T}^{\mathrm{cl}}\mathbf{C}^{\mathrm{cav}}+\cdots]_{LL'}a^0_{L'}\\&=\sum_{L'}[\mathbf{Q}^{\mathrm{cav}}\mathbf{T}^{\mathrm{cl}}(\mathbf{I}+\mathbf{P}^{\mathrm{cav}}\mathbf{T}^{\mathrm{cl}}\\&\quad+\mathbf{P}^{\mathrm{cav}}\mathbf{T}^{\mathrm{cl}}\mathbf{P}^{\mathrm{cav}}\mathbf{T}^{\mathrm{cl}}+\cdots)\mathbf{C}^{\mathrm{cav}}]_{LL'}a^0_{L'}\\&=\sum_{L'}[\mathbf{Q}^{\mathrm{cav}}\mathbf{T}^{\mathrm{cl}}(\mathbf{I}-\mathbf{P}^{\mathrm{cav}}\mathbf{T}^{\mathrm{cl}})^{-1}\mathbf{C}^{\mathrm{cav}}]_{LL'}a^0_{L'}.\end{aligned}\tag{37}$$

The scattering matrix of the system cavity + nanocluster, $\mathbf{T}^{\mathrm{cav+cl}}$, is the sum of Eqs. (33) and (37), i.e.,

$$\mathbf{T}^{\mathrm{cav+cl}}=\mathbf{T}^{\mathrm{cav}}+\mathbf{Q}^{\mathrm{cav}}\mathbf{T}^{\mathrm{cl}}[\mathbf{I}-\mathbf{P}^{\mathrm{cav}}\mathbf{T}^{\mathrm{cl}}]^{-1}\mathbf{C}^{\mathrm{cav}}.\tag{38}$$

The matrix $\mathbf{T}^{\mathrm{cav+cl}}$ is then incorporated within the existing layer-multiple-scattering formalism, allowing for the study of periodic metamaterials where the repeating unit is a spherical cavity containing a cluster of smaller scatterers.

## III. AN EXAMPLE

We consider a metamaterial made from air cavities in silica ($SiO_2$), where each cavity contains a cluster of 100 nonoverlapping gold (Au) nanoparticles (see Fig. 2). The positions of the gold particles within a cluster are taken from a Monte Carlo simulation of the self-organization of these particles under a spherically confining potential. All particles have the same radius, $S = 8.8$ nm; the average radius of the cluster is $S_{\mathrm{cl}} = 42.67$ nm while the cavity radius is

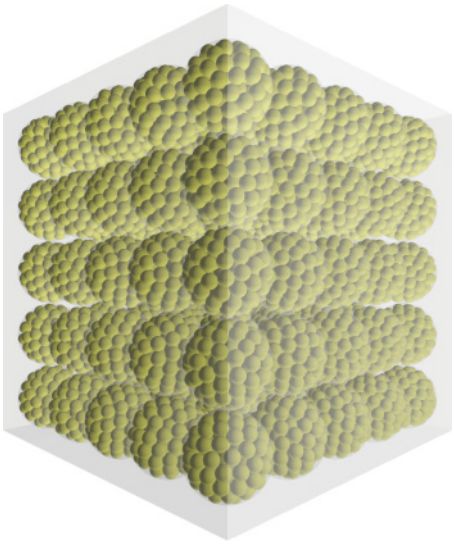

FIG. 2. (Color online) 3D orthorhombic metamaterial made of air cavities in silica containing clusters of gold nanoparticles. Each cluster consists of 100 nonoverlapping gold nanoparticles of radius $S = 8.8$ nm in a nearly close-packed arrangement, with cluster radius of 42.67 nm. Each cluster is placed at a center of a cavity of radius 44 nm. The metamaterial is viewed as a succession of (001) planes (square lattices) of clusters of gold NPs, parallel to the $xy$ plane. The lattice constant of each square lattice is $a_x = a_y = 85.22$ nm, while the lattice constant in the $z$ direction is $a_z = 87.86$ nm.

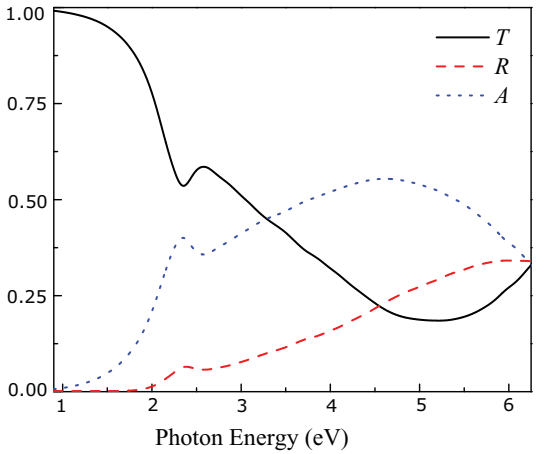


FIG. 3. (Color online) Transmittance ($T$), reflectance ($R$), and absorbance ($A$) spectra for light incident normally on a single plane of the metamaterial of Fig. 2.

$S_{\mathrm{cav}} = 44$ nm. The average interparticle distance is about 1.2 nm. The dielectric function of a single gold nanoparticle (NP) is taken from experiment,[42] with corrections accounting for the electron scattering at the boundaries of a nanoparticle [see Eqs. (3) and (4) of Ref. 43]. The metamaterial is a slightly elongated cubic (orthorhombic) lattice viewed as a succession of 2D square lattices of the above clusters of gold NPs, parallel to the $xy$ plane (see Fig. 3). The lattice constant of the 2D square lattice is $a_x = a_y = 85.22$ nm, while the lattice constant in the $z$ direction is $a_z = 87.86$ nm.

In Fig. 3, we show the transmittance, reflectance, and absorbance spectra for light incident normally on a single plane of cavities of gold clusters. The nanoparticles are small enough (8.8-nm radius) so that taking into account only the dipole terms ($l_{\max} = 1$) in the angular-momentum representation suffices for achieving convergence in the absorption spectra.[44] However, as the size of the nanoparticles increases, more terms in the angular-momentum expansion (higher-order multipoles) might be needed for a converged absorption spectra,[45,46] but not as many as required for having accurate results of quantities related with the near field. In the plane-wave expansion of the EM field,[8] we have considered 21 reciprocal-lattice vectors.

As is evident from Fig. 3, a distinct local maximum of the absorbance spectrum around 2.35 eV stems from the surface plasmon resonance of a single gold nanoparticle. Above this frequency, the absorbance spectrum exhibits a second, much broader maximum (the corresponding transmittance curve shows a broad minimum). As is evident from Fig. 4, for metamaterial slabs with more than one plane of clusters of gold nanoparticles, the absorbance curve increases dramatically: the two maxima observed for a single plane (Fig. 3) merge to a broad plateau for sufficiently thick slabs (eight planes or more; see Fig. 4).

In Fig. 5, we compare the absorption properties with different metamaterial designs in order to assess the effect of the cavity (containing the nanoparticles). From Fig. 5, it is evident that for a single plane of clusters of gold nanoparticles, light absorption is more efficient in the case where the nanoparticles are surrounded by the silica host, i.e., when they are *not* contained within a cavity. We also note that this metamaterials design (i.e., lattice of clusters of gold

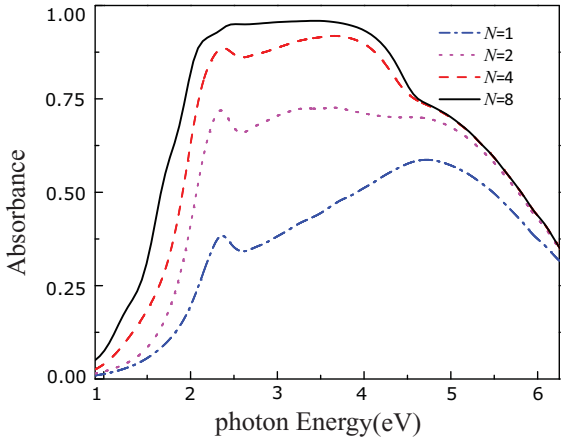


FIG. 4. (Color online) Absorbance spectra for light incident normally on finite slabs of the metamaterial of Fig. 3 of various thicknesses (numbers of planes), as shown in the legend.

nanoparticles inside silica) is a much more efficient absorber compared to a lattice of single gold nanoparticles of the equivalent radius of 42.67 nm (the same as the average radius of a cluster of 100 8.8-nm gold nanoparticles). And this is the case despite the fact that a (inhomogeneous) cluster of nanoparticles contains much less gold mass than homogeneous nanoparticles of the same radius. For the case where the nanoparticles are suspended in air, the overall absorption capability of both metamaterial designs is more or less the same. It is worth noting that, as shown in the inset of Fig. 5, even if we assume that the loss factor of a 42.67-nm gold particle is the same as

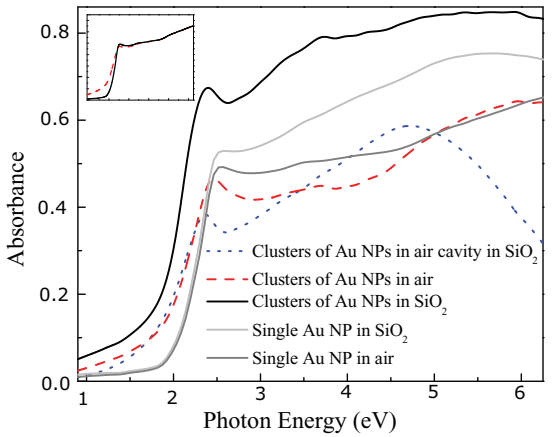


FIG. 5. (Color online) Absorbance spectra for light incident normally on a single plane of a metamaterial of clusters of gold nanoparticles embedded in a silica matrix (solid line), in air (dashed line), and inside an air cavity in silica (dotted line, which is the same as the corresponding line of Fig. 2). All three lines correspond to the same cluster of gold nanoparticles. The gray lines refer to a plane whose lattice sites are occupied by a single gold nanoparticle with the same radius as the average radius (42.67 nm) of a cluster of gold nanoparticles. The light (dark) gray line refers to the case where the nanoparticle is embedded in silica (air). Inset: The solid line is the same as the dark gray line of the main figure, while the dashed line refers to the case where the loss factor of a gold nanoparticle of radius 42.67 nm has been taken the same as the loss factor of a gold nanoparticle of radius 8.8 nm.

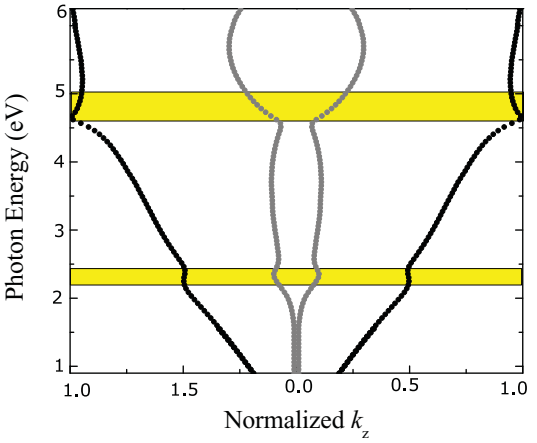


FIG. 6. (Color online) Complex frequency band structure normal to the (001) surface of the orthorhombic metamaterial of Fig. 2. The black [gray] lines correspond to $\Re k_z = \Re k_z(\omega)$ [$\Im k_z = \Im k_z(\omega)$]. The shaded regions refer to the case where $\Re n_{eff} < 0$.

that of a 8.8-nm particle (which, of course, is not true since losses due to the scattering at the boundary of the particle increase with decreasing particle radius), the corresponding absorbance spectrum does not differ much from the case where the correct loss factor for the 42.67-nm spheres has been taken into account. This implies that the efficient light absorption in the metamaterial of clusters of gold nanoparticles in silica is due to the inhomogeneous nature of the scattering element (cluster of spheres), as well as due to the strong coupling among the 8.8-nm nanoparticles, which is also heralded by the presence of a dielectric host (silica in our case) instead of air.

Finally, we examine the presence of regions with a negative refractive index, $n_{\text{eff}} < 0$. In order to do so, we have calculated the complex band structure (dispersion lines) normal to the (001) surface for the (infinitely periodic) metamaterial of Fig. 2 (air cavities+gold nanoparticles within the silica matrix). Figure 6 shows the real [$\Re k_z = \Re k_z(\omega)$] and imaginary [$\Im k_z = \Im k_z(\omega)$] dispersion lines of the above metamaterial. We identify two spectral regions (shaded areas in Fig. 6) where anomalous dispersion occurs, i.e., $\partial\omega/\partial\Re k_z < 0$. The latter would signify the occurrence of NRI if it had not been for the significant amount of losses[47] inherent in the gold nanoparticles comprising the metamaterial under study.

## IV. CONCLUSIONS

We have presented a layer-multiple-scattering method for the study of metamaterials realized as 2D or 3D lattices of cavities containing clusters of nanoparticles. It is a rigorous electrodynamic theory since it takes into account all the multiple-scattering processes experienced by light, which involve scattering within the cluster of nanoparticles, between the cluster and the cavity boundaries, and among the clusters of nanoparticles within the metamaterial. The method has been applied to the case of a lattice of air pores in silicon containing clusters of gold nanoparticles. Thick slabs of the above metamaterial act as highly efficient absorbers within the spectral region of 2–4.5 eV, while, at the same time, exhibiting anomalous dispersion over narrow spectral regions.

**ACKNOWLEDGMENTS**

The research leading to these results has received funding from the European Union's Seven Framework Programme (FP7/2007-2013) under Grant No. 228455-NANOGOLD (Self-organized Nanomaterials for Tailored Optical and Electrical Properties).

**APPENDIX**

The matrix $\Omega$ for a vector field is given by[6,39]

$$\Omega^{nn'}_{Elm;El'm'} = \Omega^{nn'}_{Hlm;Hl'm'} = (\psi_l\psi_{l'})^{-1}\big[2\alpha_l^{-m}\alpha_{l'}^{-m'}G_{l'm'-1;lm-1}(\mathbf{R}_{nn'};q_h) + mm'G_{l'm';lm}(\mathbf{R}_{nn'};q_h) + 2\alpha_l^{m}\alpha_{l'}^{m'}G_{l'm'+1;lm+1}(\mathbf{R}_{nn'};q_h)\big], \tag{A1}$$

$$\Omega^{nn'}_{Hlm;El'm'} = -\Omega^{nn'}_{Elm;Hl'm'} = (2l+1)(\psi_l\psi_{l'})^{-1}\big[-2\alpha_{l'}^{-m'}\gamma_l^{m}G_{l'm'-1;l-1m-1}(\mathbf{R}_{nn'};q_h) + m'\zeta_l^{m}G_{l'm';l-1m}(\mathbf{R}_{nn'};q_h) + 2\alpha_{l'}^{m'}\gamma_l^{-m}G_{l'm'+1;l-1m+1}(\mathbf{R}_{nn'};q_h)\big], \tag{A2}$$

where

$$\psi_l = \sqrt{l(l+1)}, \tag{A3}$$

$$\alpha_l^m = \tfrac{1}{2}[(l-m)(l+m+1)]^{1/2}, \tag{A4}$$

$$\gamma_l^m = \tfrac{1}{2}[(l+m)(l+m-1)]^{1/2}/[(2l-1)(2l+1)]^{1/2}, \tag{A5}$$

$$\zeta_l^m = [(l+m)(l-m)]^{1/2}/[(2l-1)(2l+1)]^{1/2}. \tag{A6}$$

$G_{LL'}(\mathbf{R}_{nn'};q_h)$ transforms an outgoing scalar spherical wave about $\mathbf{R}_{n'}$ to a series of incoming scalar spherical waves around $\mathbf{R}_n$. It is given by

$$G_{lm;l'm'}(\mathbf{R}_{nn'};q_h) = 4\pi\sum_{l''m''}(-1)^{(l-l'-l'')/2}(-1)^{m'+m''}B_{lm}(l''m'';l'm')h^+_{l''}(q_hR_{nn'})Y_{l''-m''}(\hat{\mathbf{R}}_{nn'}), \tag{A7}$$

with

$$B_{lm}(l''m'';l'm') = \int d\Omega Y_{lm}(\hat{\mathbf{r}})Y_{l'-m'}(\hat{\mathbf{r}})Y_{l''m''}(\hat{\mathbf{r}}). \tag{A8}$$

$Y_{lm}(\hat{\mathbf{r}})$ are the usual scalar spherical harmonics.[37]

The matrix $\Xi$ for a vector field is given by[6,39]

$$\Xi^{nn'}_{Elm;El'm'} = \Xi^{nn'}_{Hlm;Hl'm'} = (\psi_l\psi_{l'})^{-1}\big[2\alpha_l^{-m}\alpha_{l'}^{-m'}\xi_{l'm'-1;lm-1}(\mathbf{R}_{nn'};q_h) + mm'\xi_{l'm';lm}(\mathbf{R}_{nn'};q_h) + 2\alpha_l^{m}\alpha_{l'}^{m'}\xi_{l'm'+1;lm+1}(\mathbf{R}_{nn'};q_h)\big], \tag{A9}$$

$$\Xi^{nn'}_{Hlm;El'm'} = -\Xi^{nn'}_{Elm;Hl'm'} = (2l+1)(\psi_l\psi_{l'})^{-1}\big[-2\alpha_{l'}^{-m'}\gamma_l^{m}\xi_{l'm'-1;l-1m-1}(\mathbf{R}_{nn'};q_h) + m'\zeta_l^{m}\xi_{l'm';l-1m}(\mathbf{R}_{nn'};q_h) + 2\alpha_{l'}^{m'}\gamma_l^{-m}\xi_{l'm'+1;l-1m+1}(\mathbf{R}_{nn'};q_h)\big]. \tag{A10}$$

$\xi_{LL'}(\mathbf{R}_{nn'};q_h)$ transforms an outgoing (incoming) scalar spherical wave about $\mathbf{R}_{n'}$ to a series of outgoing (incoming) scalar spherical waves around $\mathbf{R}_n$ [see Eqs. (25) and (26)]. It is given by

$$\xi_{lm;l'm'}(\mathbf{R}_{nn'};q_h) = 4\pi\sum_{l''m''}(-1)^{(-l+l'+l'')/2}(-1)^{m'+m''}B_{lm}(l''m'';l'm')j_{l''}(q_hR_{nn'})Y_{l''-m''}(\hat{\mathbf{R}}_{nn'}). \tag{A11}$$

*vyannop@upatras.gr


[1] A. Gonis and W. H. Butler, *Multiple Scattering in Solids* (Springer, New York, 2000).

[2] X. Wang, X.-G. Zhang, Q. Yu, and B. N. Harmon, Phys. Rev. B **47**, 4161 (1993).

[3] A. Moroz, Phys. Rev. B **51**, 2068 (1995).

[4] J. B. Pendry, *Low Energy Electron Diffraction* (Academic, London, 1974).

[5] A. Modinos, *Field, Thermionic, and Secondary Electron Emission Spectroscopy* (Plenum, New York, 1984).

[6] A. Modinos, Physica A **141**, 575 (1987).

[7] N. Stefanou, V. Karathanos, and A. Modinos, J. Phys. Condens. Matter **4**, 7389 (1992).

[8] N. Stefanou, V. Yannopapas, and A. Modinos, Comput. Phys. Commun. **113**, 49 (1998); N. Stefanou, V. Yannopapas, and A. Modinos, *ibid*. **132**, 189 (2000).

[9] I. E. Psarobas, N. Stefanou, and A. Modinos, Phys. Rev. B **62**, 278 (2000).

[10] E. Yablonovitch, Phys. Rev. Lett. **58**, 2059 (1987).

[11] S. John, Phys. Rev. Lett. **58**, 2486 (1987).

[12] J. B. Pendry, A. J. Holden, D. J. Robbins, and W. J. Stewart, IEEE Trans. Microwave Theory Tech. **47**, 2075 (1999).

[13] J. B. Pendry, Phys. Rev. Lett. **85**, 3966 (2000).

[14] M. C. K. Wiltshire, J. B. Pendry, I. R. Young, D. J. Larkman, D. J. Gilderdale, and J. V. Hajnal, Science **291**, 849 (2001).

[15] D. Schurig, J. J. Mock, B. J. Justice, S. A. Cummer, J. B. Pendry, A. F. Starr, and D. R. Smith, Science **314**, 5801 (2006).

[16] N. I. Landy, S. Sajuyigbe, J. J. Mock, D. R. Smith, and W. J. Padilla, Phys. Rev. Lett. **100**, 207402 (2008).

[17] S. O'Brien and J. B. Pendry, J. Phys. Condens. Matter **14**, 4035 (2002).

[18] K. C. Huang, M. L. Povinelli, and J. D. Joannopoulos, Appl. Phys. Lett. **85**, 543 (2004).

[19] C. L. Holloway, E. F. Kuester, J. Baker-Jarvis, and P. Kabos, IEEE Trans. Antennas Propag. **51**, 2596 (2003).

[20] V. Yannopapas and A. Moroz, J. Phys. Condens. Matter **17**, 3717 (2005).

[21] M. S. Wheeler, J. S. Aitchison, and M. Mojahedi, Phys. Rev. B **72**, 193103 (2005).

[22] M. S. Wheeler, J. S. Aitchison, and M. Mojahedi, Phys. Rev. B **73**, 045105 (2006).

[23] L. Jylhä, I. Kolmakov, S. Maslovski, and S. Tretyakov, J. Appl. Phys. **99**, 043102 (2006).

[24] T. G. MacKay and A. Lakhtakia, J. Appl. Phys. **100**, 063533 (2006).

[25] V. Yannopapas and N. V. Vitanov, Phys. Rev. B **74**, 193304 (2006).

[26] V. Yannopapas, Phys. Rev. B **75**, 035112 (2007).

[27] A. G. Kussow, A. Akyurtlu, A. Semichaevsky, and N. Angkawisittpan, Phys. Rev. B **76**, 195123 (2007).

[28] C. W. Qiu and L. Gao, J. Opt. Soc. Am. B **25**, 1728 (2008).

[29] Q. Zhao, J. Zhou, F. Zhang, and D. Lippens, Mater. Today **12**, 60 (2009).

[30] W. T. Doyle, Phys. Rev. B **39**, 9852 (1989).

[31] R. Ruppin, Opt. Commun. **182**, 273 (2000).

[32] C. Rockstuhl, F. Lederer, C. Etrich, T. Pertsch, and T. Scharf, Phys. Rev. Lett. **99**, 017401 (2007).

[33] Q. Wu and W. Park, Appl. Phys. Lett. **92**, 153114 (2008); W. Park and Q. Wu, Solid State Commun. **146**, 221 (2008).

[34] H. J. Lee, Q. Wu, and W. Park, Opt. Lett. **34**, 443 (2009).

[35] V. A. Tamma, J. H. Lee, Q. Wu, and W. Park, Appl. Opt. **49**, A11 (2010).

[36] G. Gantzounis and N. Stefanou, Phys. Rev. B **73**, 035115 (2006).

[37] J. D. Jackson, *Classical Electrodynamics* (Wiley, New York, 1975).

[38] C. F. Bohren and D. R. Huffman, *Absorption and Scattering of Light by Small Particles* (Wiley, New York, 1983).

[39] R. Sainidou, N. Stefanou, and A. Modinos, Phys. Rev. B **69**, 064301 (2004).

[40] V. Yannopapas and N. V. Vitanov, Phys. Rev. B **75**, 115124 (2007).

[41] M. Inoue and K. Ohtaka, J. Phys. Soc. Jpn. **52**, 3853 (1983); H. Xu, E. J. Bjerneld, M. Käll, and L. Börjesson, Phys. Rev. Lett. **83**, 4357 (1999); H. Xu, J. Aizpurua, M. Käll, and P. Apell, Phys. Rev. E **62**, 4318 (2000); H. Xu and M. Käll, Phys. Rev. Lett. **89**, 246802 (2002); H. Xu, J. Opt. Soc. Am. A **21**, 804 (2004); K. Zhao, H. Xu, B. Gu, and Z. Zhang, J. Chem. Phys. **125**, 081102 (2006); Z. Li and H. Xu, J. Quantum Spectrosc. Radiat. Transfer **103**, 394 (2007).

[42] R. B. Johnson and R. W. Christy, Phys. Rev. B **6**, 4370 (1972).

[43] V. Yannopapas, Phys. Rev. B **73**, 113108 (2006).

[44] V. M. Shalaev, *Nonlinear Optics of Random Media: Fractal Composites and Metal-Dielectric Films* (Springer, Heidelberg, 2000).

[45] H. Xu, Phys. Lett. A **312**, 411 (2003).

[46] H. Xu, E. J. Bjerneld, J. Aizpurua, P. Apell, L. Gunnarsson, S. Petronis, B. Kasemo, C. Larsson, F. Höök, and M. Käll, Proc. SPIE **4258**, 35 (2011).

[47] V. Yannopapas, Opt. Commun. **282**, 4152 (2009).